



The Influence of Tool Texture on Friction and Lubrication in Strip Reduction Testing

Sulaiman, Mohd Hafis Bin; Christiansen, Peter; Bay, Niels Oluf

Published in:
Lubricants

Link to article, DOI:
[10.3390/lubricants5010003](https://doi.org/10.3390/lubricants5010003)

Publication date:
2017

Document Version
Publisher's PDF, also known as Version of record

[Link back to DTU Orbit](#)

Citation (APA):
Sulaiman, M. H. B., Christiansen, P., & Bay, N. O. (2017). The Influence of Tool Texture on Friction and Lubrication in Strip Reduction Testing. *Lubricants*, 5(1), [3]. <https://doi.org/10.3390/lubricants5010003>

General rights

Copyright and moral rights for the publications made accessible in the public portal are retained by the authors and/or other copyright owners and it is a condition of accessing publications that users recognise and abide by the legal requirements associated with these rights.

- Users may download and print one copy of any publication from the public portal for the purpose of private study or research.
- You may not further distribute the material or use it for any profit-making activity or commercial gain
- You may freely distribute the URL identifying the publication in the public portal

If you believe that this document breaches copyright please contact us providing details, and we will remove access to the work immediately and investigate your claim.



Article

The Influence of Tool Texture on Friction and Lubrication in Strip Reduction Testing

Mohd Hafis Sulaiman ^{1,2,*}, Peter Christiansen ¹ and Niels Bay ¹

¹ Department of Mechanical Engineering, Technical University of Denmark, DK-2800 Kgs. Lyngby, Denmark; petc@mek.dtu.dk (P.C.); nbay@mek.dtu.dk (N.B.)

² Mechanical Engineering Programme, Universiti Malaysia Perlis, 02600 Arau, Perlis, Malaysia

* Correspondence: mhafsul@mek.dtu.dk; Tel.: +45-4525-2144

Academic Editor: James E. Krzanowski

Received: 28 October 2016; Accepted: 4 January 2017; Published: 17 January 2017

Abstract: While texturing of workpiece surfaces to promote lubrication in metal forming has been applied for several decades, tool surface texturing is rather new. In the present paper, tool texturing is studied as a method to prevent galling. A strip reduction test was conducted with tools provided with shallow, longitudinal pockets oriented perpendicular to the sliding direction. The pockets had small angles to the workpiece surface and the distance between them were varied. The experiments reveal that the distance between pockets should be larger than the pocket width, thereby creating a topography similar to flat table mountains to avoid mechanical interlocking in the valleys; otherwise, an increase in drawing load and pick-up on the tools are observed. The textured tool surface lowers friction and improves lubrication performance, provided that the distance between pockets is 2–4 times larger than the pocket width. Larger drawing speed facilitates escape of the entrapped lubricant in the pockets. Testing with low-to-medium viscosity oils leads to a low sheet roughness on the plateaus, but also local workpiece material pick-up on the tool plateaus. Large lubricant viscosity results in higher sheet plateau roughness, but also prevents pick-up and galling.

Keywords: tool surface texture; lubricant entrapment; strip drawing test

1. Introduction

The application of surface texturing to facilitate lubrication in engineering applications such as bearings [1], reciprocating contacts [2], and concentrated sliding contacts [3] is well known. The use of tailored workpiece surfaces in sheet metal forming to improve tribological conditions has been the state of the art since the 1990s [4,5]. Studies of the lubrication mechanisms through transparent tools using mesoscopic pockets in the workpiece surface have shown that the workpiece surface topography facilitates lubrication by micro-plasto-hydrodynamic lubrication [6,7]. In industrial applications, tailored sheet surfaces are made by skin-pass rolling in the final rolling step after annealing using large rolls roughened by shot blast texturing (SBT) or electro discharge texturing (EDT) [8]. One drawback is the problem of reproducing the surfaces in large-scale sheet production due to wear of the textured roll surfaces. Aside from this drawback, there are economic considerations and the fact that the technique is less feasible in multistage operations, since the pockets are flattened out after the first forming operation [9].

The texturing of tool surfaces would be more feasible in large-scale production and multi-stage sheet stamping operations, since a textured tool surface can be utilized for thousands of workpiece components. A few tests of surface engineered deep drawing tools [10,11] have shown very promising results, indicating that tailored tool surfaces may provide mechanical lubrication systems which can function instead of chemical ones, and thereby replace environmentally hazardous lubricants with environmentally benign ones. In order to ensure the successful design of such tailored tool surfaces,

it is important to understand the influence of surface texture parameters on friction and lubrication in metal forming. Manufacturing of the tailored tool surfaces into a table mountain-like structure with flat plateaus and neighbouring flat bottomed valleys can be obtained by combined grinding, milling, and polishing of tools [12,13]. A small pocket angle towards the workpiece surface facilitates escape of the trapped lubricant in the pockets, which increases the tool life [14]. These effects can be enhanced by utilizing transverse roughness profiles and oblong pockets oriented transverse to the sliding direction. In this way, lubricant entrapment is promoted, which can lead to low friction and prevent galling by micro-plasto-hydrodynamic lubrication [15,16]. In addition, larger sliding speed reduces the tendencies of mechanical gripping effects of the workpiece into the pockets as the normal pressures increases [17].

The present paper studies textured tools in strip reduction with a focus on a small pocket angle, shallow pocket depth, and oblong pockets oriented perpendicular to the sliding direction, with varying distances between the pockets.

2. Test Setup

Figure 1 shows the strip reduction test equipment applied, whereas Figure 2 shows a schematic of the test setup with the textured tool. The front part of each workpiece strip was flattened by rolling, in order to grip the workpiece. The reduction r in each test was 15%, which emulates an ironing operation in aluminium can production. Two different drawing speeds ($v = 240$ and 65 mm/s) were applied with four different tool surfaces, as described in the following. The high and low drawing speeds were intended to identify the possible influence of a micro-plasto-hydrodynamic lubrication mechanism.

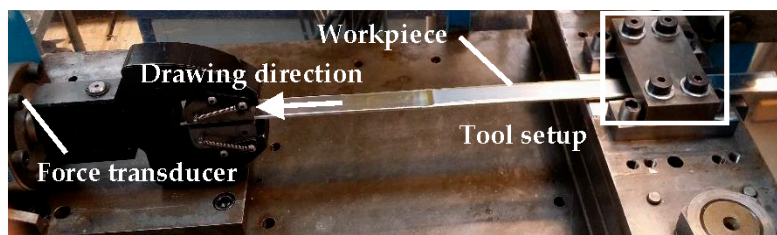


Figure 1. The strip reduction test equipment.

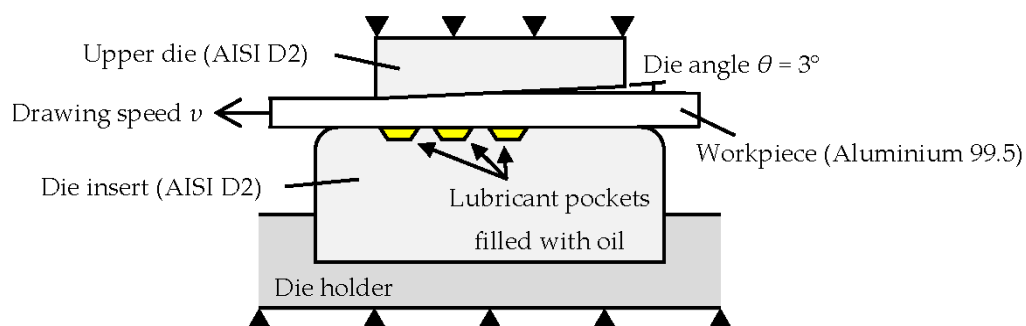


Figure 2. Schematic of the test with textured tool surface. The black triangles stand for a fixed support (a fixed table press, as shown in Figure 1).

3. Manufacture of Surface Textures

A great number of surface texturing techniques are available for the texturing of hard tool materials, such as combined milling, grinding, and manual polishing [12], chemical etching [15], rolling ball indentation [17], and laser radiation [18,19]. In this study, high-speed hard machining combined with manual polishing was chosen.

Figure 3 shows the die insert consisting of a deformation region ($X \times Y = 11.5 \times 20 \text{ mm}^2$), and a transverse pocket length $y = 16 \text{ mm}$. Two surface texture features are important parameters to promote the micro-hydrodynamic lubrication mechanism [20]; these are (1) small pocket angle γ and (2) shallow pocket depth d , see Figure 4. The pocket angle γ and the pocket depth d were chosen to be 5° and 0.01 mm , respectively. Table 1 lists the surface texture parameters as calculated by Equations (1) and (2). A TiA70 coated milling tool having a two-flute solid carbide ball-nose and a radius R of 1.25 mm was used for machining the transverse flat-bottomed lubricant pockets in the surface of the hardened tool.

$$\tan \gamma = \frac{d}{a} \quad (1)$$

$$R^2 = a^2 + H^2 = a^2 + (R - d)^2 \quad (2)$$

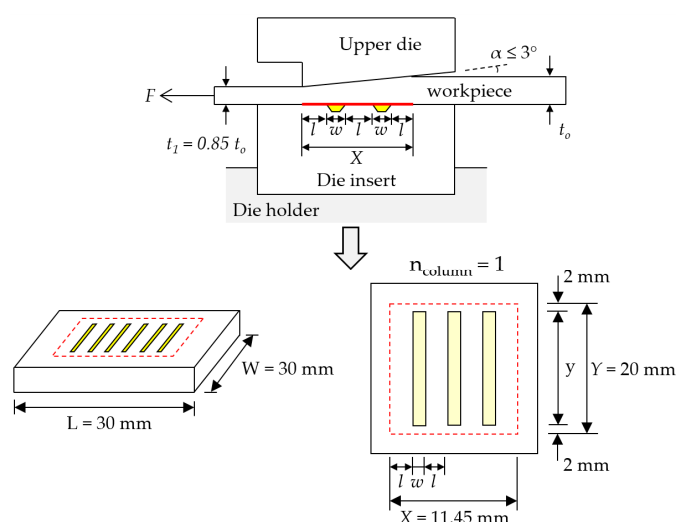


Figure 3. Texturing parameters: distance, depth, width, and number of pockets. The red dotted frame shows the contact region between textured features and workpiece surface. $n_{\text{column}} = 1$ is number of grooves in column position.

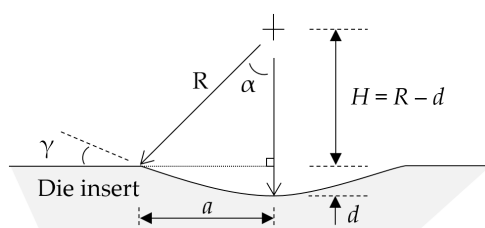


Figure 4. Selection of milling tool based on lubricant pocket geometry.

Table 1. Surface texture parameters.

Parameters	Value		
Pocket angle γ ($^{\circ}$)	5		
Pocket width $w = 2a$ (mm)	0.23		
Pocket depth d (mm)	0.01		
Pocket ratio d/w	0.05		
Distance between pockets l (mm)	$1 \times w$	$2 \times w$	$4 \times w$
Number of pockets—row n_{row}	25	16	10
Number of pockets—column n_{column}	1	1	1
Initial pocket volume V_0 (mm 3)	0.61	0.39	0.24
Contact area ratio (A_{r0}/A_0) (%)	60	74	84

The process sequence for the manufacture of a textured tool surface started with the plane tool surface being milled to $Ra = 0.14 \mu\text{m}$ on the departments five-axis high speed milling machine, Mikron HSM 400U LP (GF Machining Solutions, Odense, Denmark). After this, the transverse pocket geometry was machined with the previously mentioned milling tool running at 42,000 rpm and a feed of 600 mm/min. Figure 5 represents the result, measured pockets of nominal dimensions: length $y = 16 \text{ mm}$, angle $\gamma = 5^\circ \pm 0.5^\circ$, width $w = 0.23 \pm 0.1 \text{ mm}$, depth $d = 7 \pm 1 \mu\text{m}$, and distance between pockets of $x = 0.23, 0.46$, and 0.92 mm . Subsequent polishing of the tool surfaces were done in three steps with water based polycrystalline diamonds of grain sizes 3, 1, and $0.25 \mu\text{m}$, resulting in a final roughness $Ra = 0.01\text{--}0.03 \mu\text{m}$. The upper die and die insert surfaces were polished down to $Ra = 0.01 \mu\text{m}$. The pocket depths were reached within the tolerance gap, whereas the pocket angles turned out to be somewhat smaller than the target value. However, this only promotes the micro-hydrodynamic lubrication mechanism and prevents mechanical interlocking.

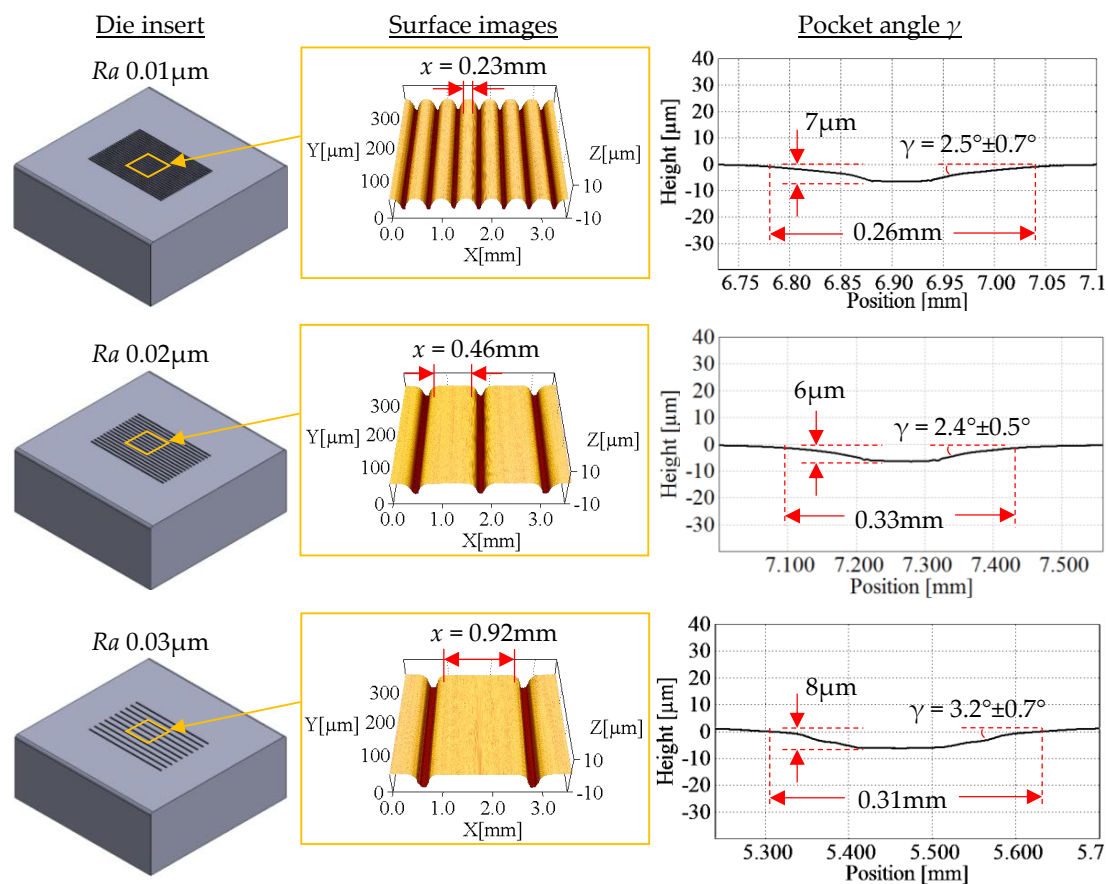


Figure 5. Manufacture of textured tools concentrating on pocket depth d and pocket angle γ .

4. Test Materials

4.1. Tool Material

The tool material was made of AISI D2 cold work tool steel (Uddeholm AB, Hagfors, Sweden), a high carbon, high chromium tool steel alloyed with molybdenum and vanadium. The tools were through-hardened and tempered to 60 HRC before the surface texturing procedure described above. The tool material is feasible for the forming of aluminium sheet material, due to high wear resistance, high compressive yield strength, and resistance towards pick-up of ductile materials like pure aluminium. It is furthermore easy to remove possible pick-up of aluminium by etching in a warm sodium hydroxide solution.

4.2. Workpiece Material

The workpiece material was a commercially pure Al 99.5, H111 (Metal service, Horsens, Denmark) with dimensions 480 mm × 20 mm × 4 mm. The 4 mm sheet thickness ensures a sufficient deformation region (tool/workpiece contact length) for a fairly large number of pockets to be within the deformation zone. This will reduce the experimental scatter data due to the results being less sensitive to the exact number of pockets within the deformation zone. The sheet width was chosen to be large enough to ensure approximately plane strain conditions resembling ironing. The as-received workpiece surface roughness was $R_a = 0.21 \mu\text{m}$. The stress–strain curve of the material shown in Figure 6 was determined by plain strain compression testing. Figure 6 also shows a curve fit and the determined material constants according to the Voce flow curve expression.

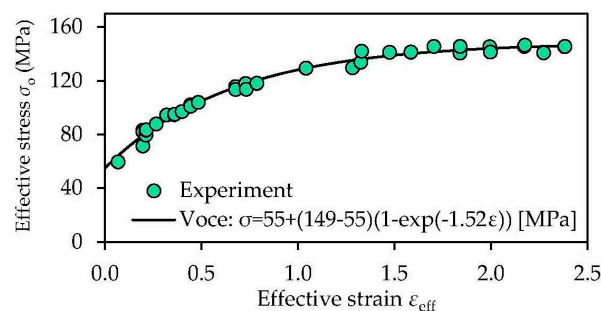


Figure 6. Voce flow curve expression for the aluminium 99.5 sheet.

4.3. Lubricants

Four different mineral oils were chosen for the experiments. Two of them—with medium and high viscosity, respectively—contained additives with boundary lubrication properties. The other two were mineral oils with no additives. One of these was high viscous oil, and the other one was a mixture of this oil and low viscous oil, giving a rather low resulting viscosity. Data on the test lubricants are listed in Table 2.

Table 2. Properties of the test lubricants.

Oil Type	Product Name	Kinematic Viscosity η [cSt @ 40 °C]
Mineral oil with additives	Rhenus LA 722086 ¹	800
Mineral oil with additives	Rhenus LA 722083 ¹	300
Pure mineral oil	CR5 Houghton Plunger ²	660
Pure mineral oil	CR5–Sun 60 ³	60

¹ From Rhenus Lub, Mönchengladbach, Germany; ² From Houghton Denmark, Sorø, Denmark; ³ 50 wt % mixture of Houghton Plunger CR5 ($\eta = 660$ cSt) and Sunoco Sun 60 ($\eta = 10$ cSt), the latter oil delivered from Sunoco, Denmark.

5. Test Procedure

The test started by cleaning the tool and workpiece surfaces from any remnants of pick-up, oil, grease, and other contaminants. Subsequently, the lubricant was applied to the different tool surfaces, after which testing was carried out. During testing, the load measurements were recorded, and the load versus time data were saved in a custom made LabView (delivered by National Instruments Denmark; Agern Allé; Denmark) program. The same procedure was repeated with the different lubricants. The plotted results were based on three to five repetitions of each parameter investigated (i.e., lubricant, drawing speed, and tool texture). Before and after testing, the tool and workpiece surfaces were scanned in a light optical microscope (LOM, Leica Microsystems, Heerbrugg, Switzerland) and measured by a tactile roughness profilometer, Taylor Hobson Form TalySurf Series 2 50i (V. Loewener, Glostrup, Denmark). The listed roughness R_a was based on an average of six measurements.

6. Results and Discussion

The drawing load reaches steady-state condition after a short time, as seen in Figures 7 and 8, showing the results for the four different lubricants at drawing speeds $v = 65$ and 240 mm/s, respectively. The influence of tool texture was significant at higher speed, while at lower speed, no load difference was observed, except that the transverse pocket with $x = 0.23$ mm led to a larger forming load, regardless of speed and lubricant applied. The small distance between the pockets ($x = 0.23$ mm) leaves no flat plateau between the pockets (see Figure 5 top). This promotes metal flow into the pockets, which will provide mechanical gripping effects of the workpiece. Marks of the die insert texture on the strip can be seen on the end of the reduction zone.

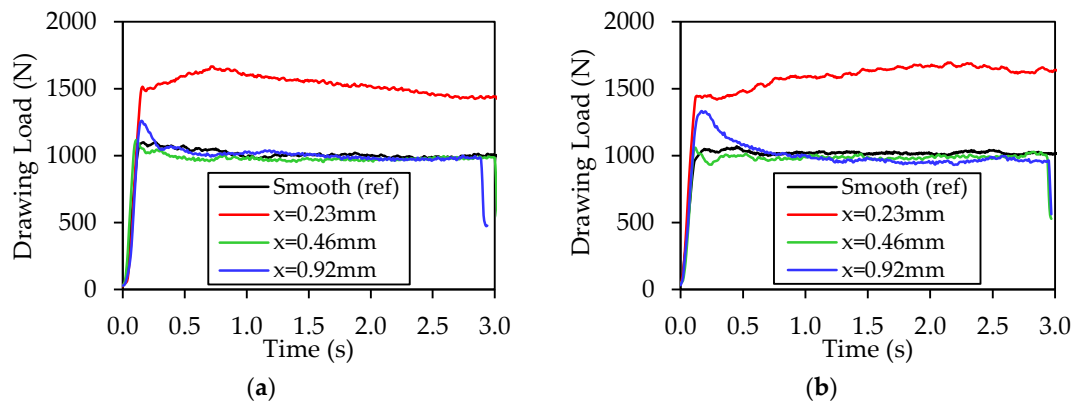


Figure 7. Forming load at speed $v = 65$ mm/s for (a) Rhenus oil $\eta = 800$ cSt; and (b) Rhenus oil $\eta = 300$ cSt.

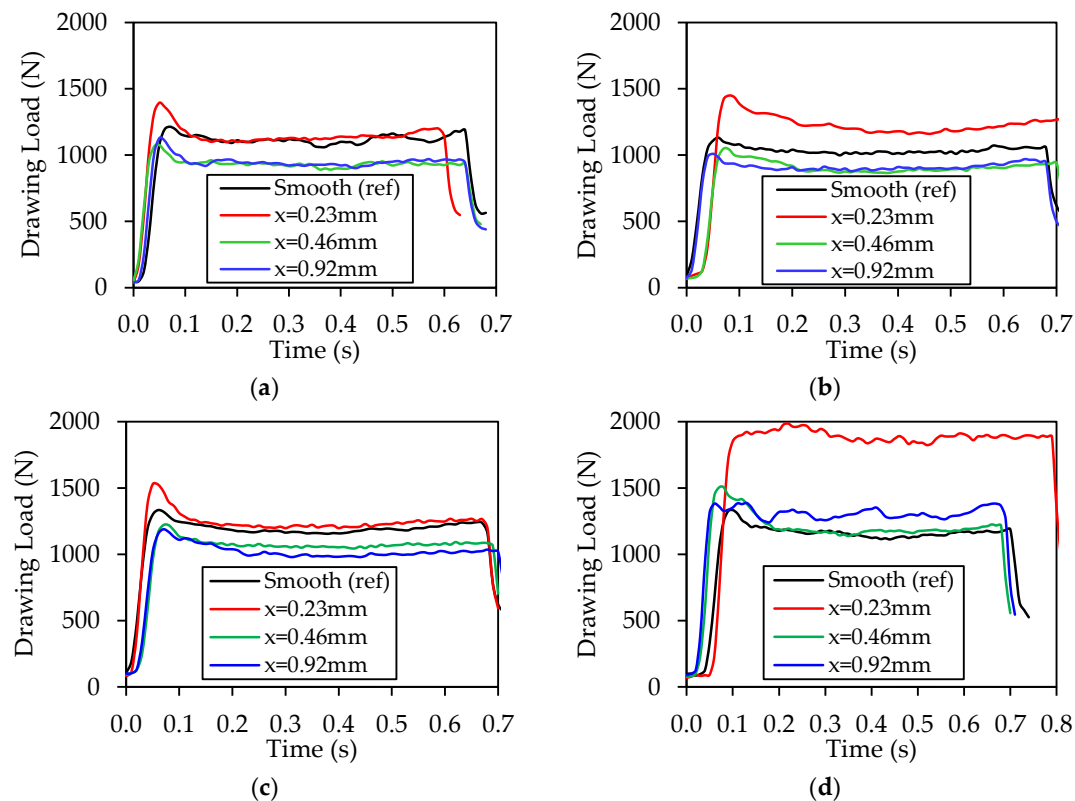


Figure 8. Forming load at speed $v = 240$ mm/s for (a) Rhenus oil $\eta = 800$ cSt; (b) Rhenus oil $\eta = 300$ cSt; (c) mineral oil CR5 $\eta = 660$ cSt; and (d) mineral oil mixtures CR5-Sun 60 $\eta = 60$ cSt.

The positive influence of high drawing speed is explained by micro-plasto-hydrodynamic lubrication, which is promoted by high sliding speed and high lubricant viscosity [21]. Since no improvements were noted on the drawing load when testing tool textures at the lower speed (65 mm/s, Figure 7), the rest of the discussion is focused on the tool texture at larger speed (240 mm/s, Figure 8). It is noticed here that the tool texture with $x = 0.46$ mm and $x = 0.92$ mm (two to four times the pocket width w) has reduced the drawing load as compared to the smooth tool surface when testing with the larger viscosity oils, while testing with the low-viscosity pure mineral oil CR5-Sun 60 had the opposite effect. This is due to the previously mentioned relationship between viscosity and micro-plasto-hydrodynamic lubrication.

Figure 9 shows that tool texture reduces the sheet roughness as compared to the smooth tool surface, regardless of the test lubricants investigated. The tool texture with pocket distance $x = 0.23$ mm gave smallest sheet roughness. It is furthermore noticed that increasing viscosity leads to increasing roughness. This may be explained by improved micro-plasto-hydrodynamic lubrication at higher viscosity, leading to effective separation between tool and workpiece on the plateaus of the tool table mountain [22]. The sheet roughness profiles shown in Figure 10 confirm this. The R_a values on the plateaus are measured by a tactile roughness profilometer, Taylor Hobson Form TalySurf Series 2 50i. They are based on an average of six measurements. R_a values for $x = 0.23$ mm and $x = 0.46$ mm could not be measured due to the small width of the plateaus.

The Rhenus oil contains additives providing a protective boundary film, which can carry the load and prevent metal-to-metal contact. This contributes to lower friction and prevents lubricant film breakdown. The additives in the Rhenus oils furthermore prevent these oils from decomposition and vaporization [23].

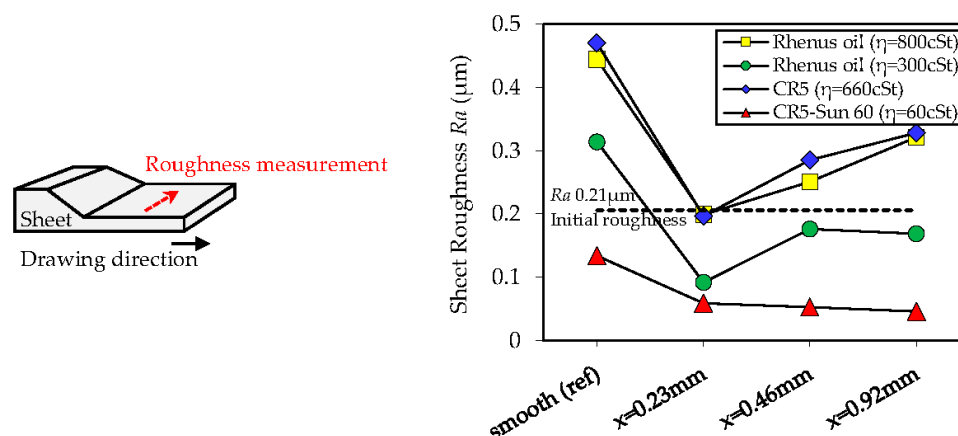


Figure 9. Sheet roughness on the plateaus at speed $v = 240$ mm/s.

Figure 11 shows images of the tool surface using light optical microscope and scanning electron microscopy with energy dispersive X-ray spectroscopy (SEM/EDX) (SEM is from JEOL, Tokyo, Japan; EDX is from Oxford Instruments, Abingdon, UK), utilized to observe possible pick-up of workpiece material on the tool surface in the contact region. Testing of the Rhenus oil with a viscosity of 800 cSt showed no sign of pick-up at all, which is explained by the complete separation between tool and workpiece surface, as evidenced in Figure 10.

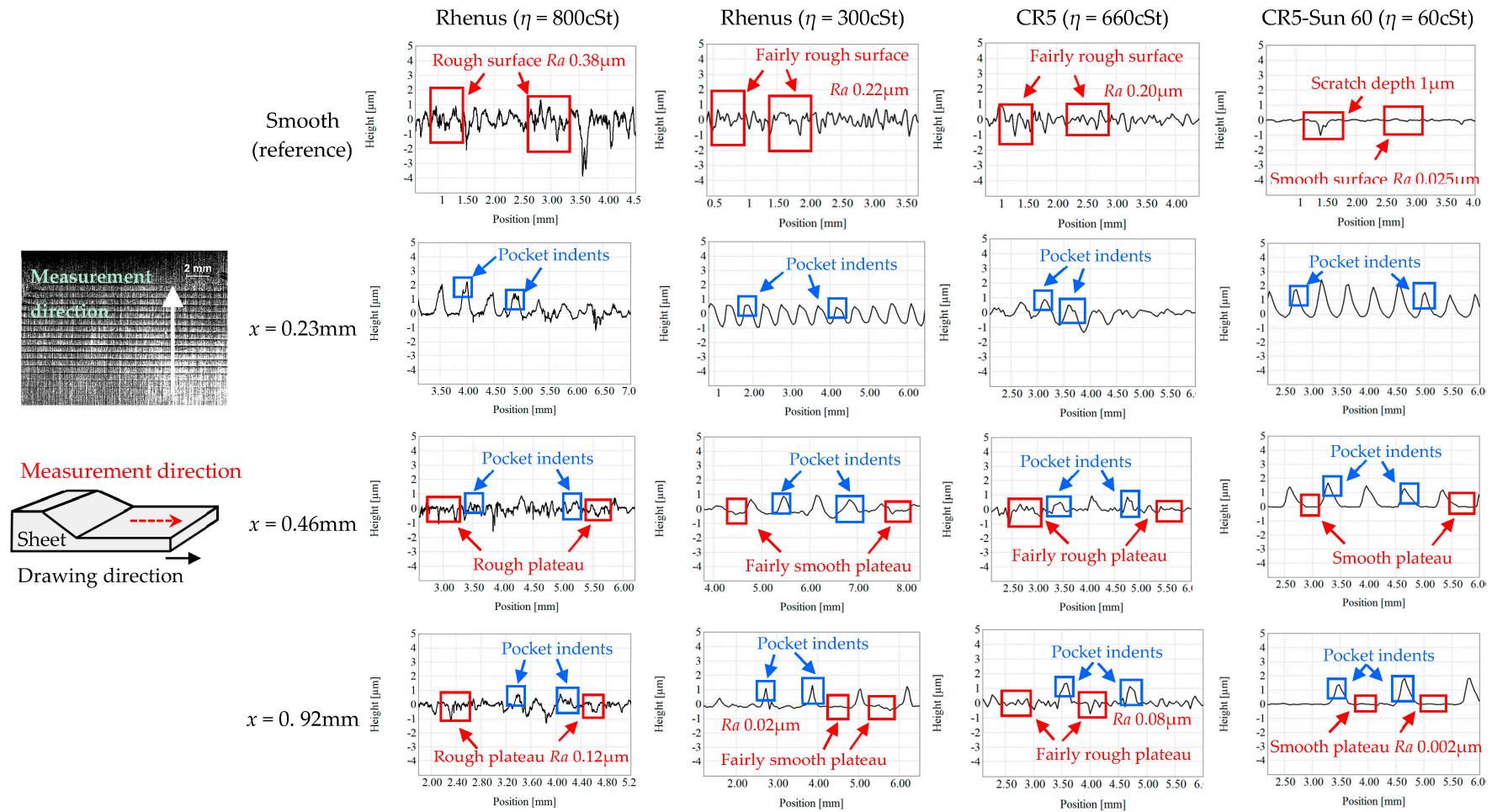


Figure 10. Roughness profiles of the sheets flowed into the pockets when testing with different tool textures and lubricants at speed $v = 240$ mm/s.

Pick-up of aluminium was observed on the plateaus of the table mountain structure, especially in the last part of the tool/workpiece contact region corresponding to a thickness reduction r close to 15%. The rectangular frames in the LOM images marked A, B, C, and D in Figure 11 indicate the approximate location of the SEM images, although the frames are larger than the SEM images. Testing of the Rhenus oil with viscosity of 300 cSt and the pure mineral oil with a viscosity of 660 cSt resulted in 0.2–1.0 wt % and 0.1–0.2 wt % pick-up, respectively, while the low viscosity CR5-Sun 60 oil resulted in an increased amount of pick-up of 0.3–17.9 wt %. This is as expected, since the low-viscosity mineral oil with no additives does not promote micro-plasto-hydrodynamic lubrication and has no boundary lubrication properties, whereas the higher viscosity Rhenus oil and the high viscosity pure mineral oil may support micro-hydrodynamic lubrication and the Rhenus oil furthermore has boundary lubricating properties. The slightly better performance of CR5 compared to the lower viscosity Rhenus oil further supports the hypothesis of micro-hydrodynamic effects.

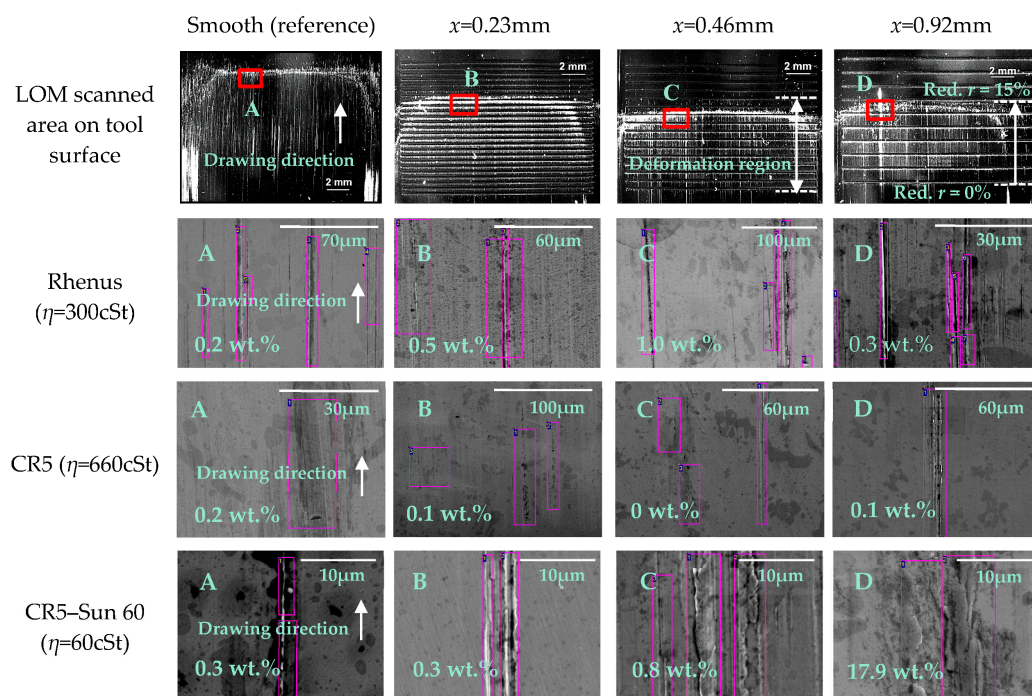


Figure 11. Pick-up occurred at the larger reduction region r of 15%. The red marked locations named A, B, C and D in the LOM micrographs are shown in larger magnification in the SEM micrographs below the first row. The purple squares indicate where the amount of pick-up was determined.

7. Conclusions

A technique to improve resistivity towards galling by applying textured tool surface topographies was investigated. Oblong shallow pockets with small pocket angles, oriented perpendicular to the sliding direction with a distance of 1–4 times the pocket width were tested. A strip reduction test, which emulates the tribological conditions in an ironing process, was used for experimental measurements of friction and determination of possible pick-up and galling. The study included testing of four different lubricants—two plain mineral oils with a low and a high viscosity, and two mineral-based oils with boundary lubrication additives having medium and high viscosity. The results confirmed that tool texture can lower friction and improve lubrication performance in comparison to that of a fine polished tool surface when the pocket distance is 2–4 times the pocket width, which ensures a table mountain structure of the tool topography. The tool textures were advantageous at greater sliding speeds, when using higher viscosity oils, which facilitate the escape of trapped lubricant by micro-plasto-hydrodynamic lubrication.

Acknowledgments: The work is supported by the Danish Council for Independent Research under grant No. DFF—4005-00130. Mohd Hafis Sulaiman would like to thank the Universiti Malaysia Perlis and the Ministry of Education, Malaysia for providing sponsorship for his PhD study at Technical University of Denmark (DTU). The authors gratefully acknowledge the support from Ermanno Ceron from Grundfos A/S; Denmark for providing the Rhenus oils. The authors are thankful for the support of the staffs and the facilities at DTU manufacturing laboratory and DTU tribology laboratory during the course of the research.

Author Contributions: Mohd Hafis Sulaiman conceived and designed the experiments under supervision of Peter Christiansen and Niels Bay; Mohd Hafis Sulaiman performed the experiments; Mohd Hafis Sulaiman analyzed the data and discussed the results with Peter Christiansen and Niels Bay; Mohd Hafis Sulaiman, Peter Christiansen and Niels Bay contributed with reagents/materials/analysis tools; Mohd Hafis Sulaiman wrote the paper; Peter Christiansen and Niels Bay revised the paper.

Conflicts of Interest: The authors declare no conflict of interest.

References

1. Ibatan, T.; Uddin, M.S.; Chowdhury, M.A.K. Recent development on surface texturing in enhancing tribological performance of bearing sliders. *Surf. Coat. Technol.* **2015**, *272*, 102–120. [[CrossRef](#)]
2. Vladescu, S.C.; Olver, A.V.; Pegg, I.G.; Reddyhoff, T. The effects of surface texture in reciprocating contacts—An experimental study. *Tribol. Int.* **2015**, *82*, 28–42. [[CrossRef](#)]
3. Bruzzone, A.A.G.; Costa, H.L.; Lonardo, P.M.; Lucca, D.A. Advances in engineered surfaces for functional performance. *CIRP Ann. Manuf. Technol.* **2008**, *57*, 750–769. [[CrossRef](#)]
4. Geiger, M.; Engel, U.; Pfestorp, M. New developments for the qualification of technical surfaces in forming processes. *Ann. CIRP* **1997**, *46*, 171–174. [[CrossRef](#)]
5. Schmoedel, D.; Prier, M.; Staevs, J. Topography deformation of sheet metal during the forming process and its influence on friction. *Ann. CIRP* **1997**, *46*, 175–178. [[CrossRef](#)]
6. Kudo, H.; Azushima, A. Direct observation of contact behaviour to interpret the pressure dependence of the coefficient of friction in sheet metal forming. *Ann. CIRP* **1995**, *1*, 209–212.
7. Bay, N.; Bech, J.L.; Andreasen, J.L.; Shimizu, I. Studies on micro plasto hydrodynamic lubrication in metal forming. In *Metal Forming Science and Practice: A State-of-the-Art Volume in Honour of Professor J.A. Schey's 80th Birthday*, 1st ed.; Lenard, J.G., Ed.; Elsevier Science Ltd.: Oxford, United Kingdom, 2002; Chapter 7; pp. 115–134.
8. Kijima, H.; Bay, N. Contact conditions in skin-pass rolling. *Ann. CIRP* **2007**, *1*, 301–306. [[CrossRef](#)]
9. Groche, P.; Stahlmann, J.; Hartel, J.; Kohler, M. Hydrodynamic effects of macroscopic deterministic surface structures in cold forging processes. *Tribol. Int.* **2009**, *42*, 1173–1179. [[CrossRef](#)]
10. Lindvall, F.; Bergstrom, J.; Krakhmalev, P.; Bay, N. The effect of grinding and polishing procedure of tool steels in sheet metal forming. In *Proceedings of the 4th International Conference on Tribology in Manufacturing Processes, (ICTMP 2010)*, Nice, France, 13–15 June 2010; Felder, E., Montmitonnet, P., Eds.; Presses des MINES: Paris, France, 2010; Volume 2, pp. 603–612.
11. Wiklund, D.; Liljebgren, M.; Berglund, J.; Bay, N.; Kjellsson, K.; Rosen, B.-G. Friction in sheet metal forming—A comparison between machined and manually polished die surfaces. In *Proceedings of the 4th International Conference on Tribology in Manufacturing Processes, (ICTMP 2010)*, Nice, France, 13–15 June 2010; Felder, E., Montmitonnet, P., Eds.; Presses des MINES: Paris, France, 2010; Volume 2, pp. 613–622.
12. Eriksen, R.S.; Arentoft, M.; Gronbak, J.; Bay, N. Manufacture of functional surfaces through combined application of tool manufacturing processes and Robot Assisted Polishing. *CIRP Ann. Manuf. Technol.* **2012**, *61*, 563–566. [[CrossRef](#)]
13. Godi, A.; Gronbak, J.; De Chiffre, L. Off-line testing of multifunctional surfaces for metal forming applications. *CIRP J. Manuf. Sci. Technol.* **2015**, *11*, 28–35. [[CrossRef](#)]
14. Popp, U.; Engel, U. Microtexturing of cold-forging tools—Influence on tool life. *Proc. Inst. Mech. Eng. B* **2006**, *220*, 27–33. [[CrossRef](#)]
15. Costa, H.L.; Hutchings, I.M. Effects of die surface patterning on lubrication in strip drawing. *J. Mater. Process. Technol.* **2009**, *209*, 1175–1180. [[CrossRef](#)]
16. Krux, R.; Homberg, W.; Kalveram, M.; Trompeter, M.; Kleiner, M.; Weinert, K. Die surface structures and hydrostatic pressure system for the material flow control in high-pressure sheet metal forming. *Adv. Mater. Res.* **2005**, *6–8*, 385–392. [[CrossRef](#)]

17. Franzen, V.; Witulski, J.; Brosius, A.; Trompeter, M.; Tekkaya, A.E. Textured surfaces for deep drawing tools by rolling. *Int. J. Mach. Tools Manuf.* **2010**, *50*, 969–976. [[CrossRef](#)]
18. Wagner, K.; Volkl, R.; Engel, U. Tool life enhancement in cold forging by locally optimized surfaces. *J. Mater. Process. Technol.* **2008**, *201*, 2–8. [[CrossRef](#)]
19. Podgornik, B.; Jerina, J. Surface topography effect on galling resistance of coated and uncoated tool steel. *Surf. Coat. Technol.* **2012**, *206*, 2792–2800. [[CrossRef](#)]
20. Shimizu, I.; Martins, P.A.F.; Bay, N.; Andreasen, J.L.; Bech, J.I. Influences of lubricant pocket geometry and working conditions upon micro lubrication mechanisms in upsetting and strip drawing. *Int. J. Surf. Sci. Eng.* **2010**, *4*, 42–54. [[CrossRef](#)]
21. Bech, J.; Bay, N.; Eriksen, M. A study of mechanisms of liquid lubrication in metal forming. *Ann. CIRP* **1998**, *47*, 221–226. [[CrossRef](#)]
22. Bech, J.I.; Bay, N.; Eriksen, M. Entrapment and escape of liquid lubricant in metal forming. *Wear* **1999**, *232*, 134–139. [[CrossRef](#)]
23. Stachowiak, G.W.; Batchelor, A.W. *Engineering Tribology*, 3rd ed.; Butterworth-Heinemann Elsevier: Oxford, UK, 2014; pp. 1–852.



© 2017 by the authors; licensee MDPI, Basel, Switzerland. This article is an open access article distributed under the terms and conditions of the Creative Commons Attribution (CC-BY) license (<http://creativecommons.org/licenses/by/4.0/>).